Simple Procedure for Polystyrene-Based Nanocomposite Preparation by Vapor-Phase-Assisted Surface Polymerization

ARTICLE *in* MACROMOLECULES · SEPTEMBER 2009

Impact Factor: 5.8 · DOI: 10.1021/ma901357p

4 AUTHORS, INCLUDING:

Yoshito Ando
Kyushu Institute of Technology
56 PUBLICATIONS **315** CITATIONS
SEE PROFILE

Takeshi Endo
Kinki University
1,126 PUBLICATIONS **16,859** CITATIONS
SEE PROFILE

DOI: 10.1021/ma901357p

Macromolecules
ARTICLE

Simple Procedure for Polystyrene-Based Nanocomposite Preparation by Vapor-Phase-Assisted Surface Polymerization

Yoshito Andou,[†] Jae-Mun Jeong,[†] Haruo Nishida,*[,‡] and Takeshi Endo*[,†]

[†]*HENKEL Research Center of Advanced Technology, Molecular Engineering Institute, Kinki University, 11-6 Kayanomori, Iizuka, Fukuoka 820-8555, Japan, and* [‡]*Eco-Town Collaborative R&D Center for the Environment and Recycling, Kyushu Institute of Technology, 2-4 Hibikino, Wakamatsu-ku, Kitakyushu, Fukuoka 808-0196, Japan*

Received June 24, 2009; Revised Manuscript Received September 1, 2009

ABSTRACT: Polystyrene (PSt)-based copolymer/montmorillonite (MMT) nanocomposites were prepared by an in situ vapor-phase-assisted surface polymerization (VASP) as a solventless method using an organically modified MMT and a free radical initiator. Simultaneous and consecutive VASP of styrene (St) and methyl methacrylate (MMA) on the premodified MMT induced the accumulation of poly(MMA-*ran*-St) and poly(MMA-*block*-St) on the MMT surface, resulting in effective intercalation and exfoliation of silicate layers. The homogeneously dispersed silicate platelets in the polymer matrices were confirmed by X-ray diffraction and transmission electron microscope analyses. An important contributor to this phenomenon must be the particular interaction between a small amount of MMA units and silicate surfaces. This approach allows the nanocomposites with accompanying intercalation and exfoliation of silicate layers to be applied to a wide range of vaporizable monomers which in the absence of this technique would be otherwise difficult to individually prepare.

Introduction

Until recently, among the nanocomposites, the polymer/montmorillonite (MMT) nanocomposite, in which silicate platelets in MMT are dispersed on a nanoscale throughout the polymer matrix, has been seen as one of the most valuable kinds of composites because this dispersion of silicate platelets gives to the nanocomposites gas barrier properties, physical strength, heat stability,[1] and a specific interfacial interaction with electric conducting polymers[2] such as polypyrrole, polyaniline, or poly(amic acid).

Homogeneous dispersion of the completely delaminated silicate layers is desirable because it ensures the maximum reinforcement of the composites. However, incompatibility between the hydrophilic layered silicates and hydrophobic polymer matrices makes it difficult to separate and disperse the individual platelets throughout polymer matrices. Therefore, to achieve exfoliation, various procedures have been devised. For example, in the preparation of polystyrene (PSt)-based nanocomposites,[3−9] procedures attempted include the uses of various initiator−MMT hybrids,[3,4] a protonated amine[5] and carboxyl terminated polystyrenes,[6] in situ bulk and solution polymerizations of styrene using coreactive organophilic montmorillonite,[7,8] and melt compounding of organophilic layered silicates and polystyrene in the presence of poly(styrene-*co*-vinyloxazoline).[9] Even though these ingenious procedures have induced the successful exfoliation of the layered silicates, the processes are troublesome and still require large amounts of solvents.[4b,10]

The vapor-phase-assisted surface polymerization (VASP) technique has been developed as the simplest method for constructing microarchitectures on solid substrate surfaces with the advantages of being solventless and precise.[11] The presence of fine gaps and spaces within the solid substrate provide an additional advantage commending use of the VASP technique in the construction of fine structured composites[12] and coatings.[13] These gaps and spaces, when wider than the size of monomer molecule, allow the vaporized monomer to diffuse and penetrate interstitially within the solid substrates. After the diffusion and adsorption on the interstitial surfaces, the monomers polymerize in a manner of "pseudo-grafting from" the substrate surfaces. Polymer chains then grow on the surfaces by filling the spaces.

Recently, a simple construction method for a vinyl polymer/clay nanocomposite by VASP of methyl methacrylate (MMA) to obtain a completely exfoliated PMMA/MMT nanocomposite was reported.[14] The VASP of MMA made the *d*-spacing of the silicate layers readily expand and consequently exfoliate to form a nanocomposite.

This VASP approach to nanocomposite construction, as well as providing the novel benefits of being a solventless process, generating high concentrations of clay in nanocomposites, and using a minimum of resources, also allows easy production of block copolymers by the exchange of a monomer vapor.[11d] This block copolymerization technique has great potential in nanocomposite production because it provides a possible solution to the intrinsic incompatibility between clay and polymer. In this paper, we designed a clay-compatible block copolymer by VASP, resulting in the formation of highly dispersed PSt-based copolymer/clay nanocomposites. The morphologies and thermal stability of the nanocomposites were also analyzed.

Experimental Section

Materials. Monomers, methyl methacrylate (MMA, 99.0%, Tokyo Chemical Industry Co., Ltd.), and styrene (St, 99%, from Wako Pure Chemical Industries, Ltd. (Wako)) were purified by distillation under reduced pressure over CaH_2 just before

*Corresponding author: Fax +81-63-695-6060, e-mail nishida@lsse.kyutech.ac.jp (H.N.); Fax +81-948-22-5706, e-mail tendo@me-henkel.fuk.kindai.ac.jp (T.E.).

 Published on Web 09/16/2009

polymerization. Initiator, 2,2′-azobis(isobutyronitrile) (AIBN, >99%), was purchased from Otsuka Chemical Inc. and crystallized from methanol. Polymerization inhibitor, 4-*tert*-butylpyrocatechol (>98%), was purchased from Wako and used as received. Substrate, organophilic montmorillonite (C18MMT, *d*-spacing 2.2 nm), which was modified with dimetylstearylammonium chloride, was used as received from Kunimine Industries Co., Ltd. All other reagents, such as acetone (>99%), chloroform ($CHCl_3$, >99.0%, HPLC grade), and methanol (>99%), were commercially obtained and purified by distillation.

Initiator intercalated C18MMT (powder, diameter <0.05 mm) was prepared in the same manner as reported elsewhere in detail.[14] Before VASP, to intercalate the initiator AIBN into the silicate layers, C18MMT (1.54 g) was pretreated with a 1 mM acetone solution (500 mL) of AIBN at a 1:30 weight ratio to C18MMT at 25 °C for 0.5 h under stirring. After the pretreatment, acetone was removed under vacuum at room temperature, resulting in the production of powdery AIBN-intercalated C18MMT (*d*-spacing 2.3 nm).[14] The pretreated C18MMT powder was stirred in $CHCl_3$ to wash out the initiators attached to outside surfaces.

Typical Procedure of Simultaneous Copolymerization. To obtain random copolymers, simultaneous copolymerization was employed. A typical simultaneous VASP of MMA and St was carried out in an H-shaped glass tube reactor with a vacuum cock. The C18MMT powder preintercalated with AIBN (100 mg) was measured into a glass pan (bottom surface area: 707 mm^2), and the glass pan was set in the bottom of one of the legs of the H-shaped glass tube reactor. Prescribed amounts of monomers—MMA and St—and inhibitor—4-*tert*-butylpyrocatechol (20 mg, 1.2×10^{-4} mol)—were introduced into the bottom of the other leg. The reactor was degassed by three freeze−pump−thaw cycles and then sealed under a saturated atmosphere of vaporized monomers. Polymerization was carried out at 70 °C for 3 h in a thermostated oven. After the reaction, the powdery sample, which had been expanded by newly intercalated polymer chains, was dried to remove the adsorbed monomers in vacuo and weighed to obtain poly(MMA-*ran*-St)/C18MMT composites. The produced powdery composites (diameter <0.1 mm) were analyzed intact with an X-ray diffractometer (XRD) to measure the *d*-spacing of the silicate layers.

Free polymers in the obtained composites were extracted using tetrahydrofuran (THF) as a good solvent of the copolymer at 80 °C for 24 h. THF solution was repeatedly filtered to ensure the removal of the clay, and then extracted polymer was precipitated with methanol. The isolated polymers were dried and analyzed by Fourier transform infrared (FTIR), ^{1}H NMR, and size-exclusion chromatography (SEC). Moreover, free homopolymers were extracted from the THF-extracted products at 80 °C for 24 h using selective solvents, i.e., cyclohexane for PSt and acetonitrile for PMMA.[11d] Characterization of fractions—copolymer and homopolymers—was carried out with ^{1}H NMR, FTIR, and SEC.

Typical Procedure for Consecutive Copolymerization. To obtain block copolymers, consecutive copolymerization was employed for VASP. The C18MMT powder, preintercalated with AIBN (100 mg), was measured into a glass pan (bottom surface area: 707 mm^2) and the glass pan then set in the bottom of one of the legs of the H-shaped glass tube reactor. MMA (2.0 mL) and 4-*tert*-butylpyrocatechol (20 mg, 1.2×10^{-4} mol) were added in the bottom of the other leg. The reactor was degassed by three freeze−pump−thaw cycles and then sealed in a saturated atmosphere of MMA. Polymerization was carried out at 60 °C for 18 h under a saturated vapor pressure of 2.34×10^4 Pa in an oven. After the first stage, the reactor was cooled to room temperature, and the remaining MMA was removed in vacuo. Next, the second monomer, St (2.0 mL), was introduced into the bottom with a syringe through the glass cock of the reactor under an Ar gas flow. The reactor was degassed again by three freeze−pump−thaw cycles and then sealed under a saturated atmosphere of St. The second stage was also carried out at 80 °C for 11 h under a saturated vapor pressure of 1.85×10^4 Pa without any additional initiator. After the reaction, the produced powdery composite on the glass pan was dried in vacuo and weighed to obtain poly(MMA-*block*-St)/C18MMT composite. The polymer was characterized in a similar way to the copolymers obtained by the simultaneous VASP.

Procedure in Solution Polymerization. A solution polymerization of St was carried out in a toluene suspension of the same AIBN pretreated C18MMT at 85 °C for 3 h. The AIBN preintercalated C18MMT powder (100 mg) was measured into a 10 mL glass tube before St (1.25 mL) and toluene (1.0 mL) were added. The reactor was degassed by three freeze−pump−thaw cycles and then sealed in a nitrogen atmosphere at normal pressure. Solution polymerization was carried out at 85 °C for 3 h in a thermostated oil bath. After polymerization, the reactor was cooled to room temperature, and the reaction mixture was diluted by THF, followed by the precipitation of the product into hexane. The precipitate was dried under a reduced pressure for 24 h at 25 °C, and the product was characterized in a similar way to the copolymers obtained by the simultaneous VASP.

Melt Processing. Melt processing of poly(MMA-*ran*-St)/C18MMT powdery composites was carried out by compression molding, in which the composites were preheated for 2 min in an oil press heated at 210 °C followed by heat-pressing for 3 min at the same temperature to obtain a thin film (thickness ca. 100 μm).

Characterization Methods. XRD patterns were obtained by using a Rigaku diffractometer equipped with a Cu Kα generator (λ = 0.1541 nm) under the following conditions: slit width, 0.30 mm; generator current, 16 mA; voltage, 30 kV; and scanning rate, 2 deg min^{-1}.

^{1}H NMR spectra were recorded on a 300 MHz JEOL AL-300 MHz spectrometer. Chloroform-*d* ($CDCl_3$) was used as a solvent. Chemical shifts were reported as δ values (ppm) relative to internal tetramethylsilane (TMS) in $CDCl_3$ unless otherwise noted. FTIR spectroscopy was performed using a JASCO FTIR 460 plus spectrometer. Transmission spectra were recorded from KBr disks, whose surfaces were coated with polymer samples from chloroform solutions.

Molecular weights of polymers were measured on a TOSOH HLC-8220 SEC system with refractive index (RI) and ultraviolet (UV, λ = 254 nm) detectors under the following conditions: TSKgel Super HM-H linear column (linearity range, 1×10^3−8×10^6; molecular weight exclusion limit, 4×10^8), THF eluent at a flow rate of 0.6 mL min^{-1}, and column temperature of 40 °C. The calibration curves for SEC analysis were obtained using polystyrene standards with a low polydispersity (5.0×10^2, 1.05×10^3, 2.5×10^3, 5.87×10^3, 9.49×10^3, 1.71×10^4, 3.72×10^4, 9.89×10^4, 1.89×10^5, 3.97×10^5, 7.07×10^5, 1.11×10^6, TOSOH Corp.).

Thermogravimetric/differential thermal analysis (TG/DTA) was performed on a TG/DTA 6200 (Seiko Instruments Inc.) under nitrogen flow (100 mL min^{-1}) with a heating rate of 10 °C min^{-1}.

Transmission electron microscopy (TEM) was carried out on a JEOL JEM-3010 transmission electron microscope with an accelerating voltage of 200 kV. For TEM measurements, the melt-processed thin films from poly(MMA-*ran*-St)/C18MMT composites were ultramicrotomed with a diamond knife.

Results and Discussion

Simultaneous Copolymerization. On the basis of the monomer reactivity ratio of St and MMA on free radical copolymerization, r_{St} and r_{MMA} have been reported as 0.52 and 0.46, respectively.[15] This means that St is introduced preferentially into copolymers. However, in the silicate interlayers

Table 1. Simultaneous VASP of St/MMA on AIBN Pre-intercalated C18MMT for 3 h at 70 °C[a]

entry	monomer ratio St/MMA (mL/mL)	polymer yield (mg)	M_n[b] ($\times 10^5$)	PDI	*d*-spacing (nm)	unit ratio in copolymer[c] [St]/[MMA]
1	2.0/0	960	10.7	2.5	3.9	
Sol-1[d]	1.25/0	120	0.3	2.8	3.4	
2	2.0/0.1	580	12.9	1.9	4.1	9.6
3	2.0/0.2	740	12.4	1.7	>4.4[e]	7.0
4	1.5/0.3	460	6.9	2.3	>4.4[e]	4.2
5	1.5/0.5	430	7.9	1.8	>4.4[e]	3.0

[a] Polymerization conditions: substrate, C18MMT (100 mg); C18MMT:AIBN = 30:1 (w/w). [b] Number-average molecular weight determined by SEC relative to polystyrene standards. [c] Calculated from ^{1}H NMR peak intensities of a singlet at 2.00−3.65 ppm (−$COOCH_3$ in MMA unit) and signals at 6.28−7.20 ppm (aromatic protons in St unit) in ^{1}H NMR spectra. [d] Polymerization in a toluene (1 mL) solution. [e] No diffraction peak in a range of 2θ = 2°−10°, which is indicative of exfoliated structure.

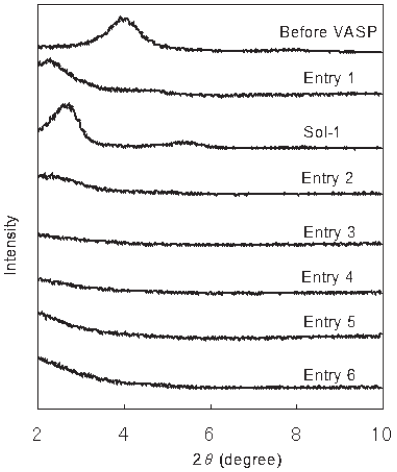

Figure 1. XRD patterns of C18MMT and PSt-based copolymer/C18MMT composites.

of organoclay, the monomer reactivity ratio may change due to differences in the affinity of monomers with the silicate layer surface. Taking into consideration the affinity, simultaneous VASP of St and MMA was carried out with various monomer feed ratios of St/MMA = 2.0/0−0.5/1.5 (mL/mL) (entries 1−5 in Table 1) in the presence of the AIBN preintercalated C18MMT powder.

VASP of St on the AIBN preintercalated C18MMT (entry 1) proceeded with gradual expansion in volume of the C18MMT producing a lump of powdery solid product, with an accompanying drastic increase in the *d*-spacing value between silicate layers to 3.9 nm, much greater than the 2.3 nm of the original AIBN preintercalated C18MMT as shown in Figure 1. This phenomenon indicates that an intercalated polymer/C18MMT nanocomposite was formed via this VASP of St, but not an exfoliated one. To determine the molecular weight of the polymeric product, a free polymeric component was dissolved with THF, and the solution was filtered repeatedly to ensure the removal of the clay. The extracted polymer was then precipitated with methanol. The number- and weight-average molecular weights, analyzed by SEC, of the isolated polymer were 1.1×10^6 and 2.7×10^6, respectively, values that are high enough for PMMA to exfoliate the silicate layers.[14]

The VASP product in entry 1 was compared with a product of a solution polymerization of St (entry Sol-1), which was carried out in a toluene suspension of the same AIBN pretreated C18MMT powder. In spite of a comparable amount of product (120 mg), the XRD profile of the product showed only a small expansion in the *d*-spacing (3.4 nm) between the silicate layers (Figure 1). These results suggest that it would be difficult to prepare a completely exfoliated PSt/clay nanocomposite either by VASP or by the solution polymerization of St under the employed conditions.

Scheme 1. Exfoliation of Silicate Layers of MMT during Simultaneous VASP Process

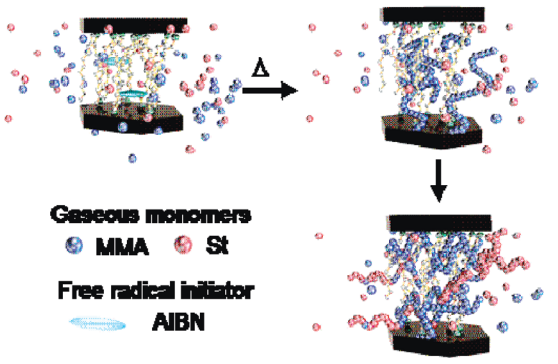

To prepare exfoliated nanocomposites, random copolymers of MMA and St were prepared by the simultaneous VASP of both monomers on the AIBN preintercalated C18MMT (entries 2−5), resulting in powdery products. The expansion of the *d*-spacing into the exfoliation of the silicate layers in the products was clearly observed with increase in the feed ratio of MMA (Figure 1). Addition of a small amount of MMA in the feed (entry 2, St/MMA = 2.0/0.1) caused a further expansion in *d*-spacing (4.1 nm) of the intercalated silicate layers. Further addition of MMA in the feed (entries 3−5) resulted in more expansion between the silicate layers in the VASP products, resulting in a *d*-spacing of greater than 4.4 nm at the limit of the 2θ value (2.0°) measurable with the XRD.

From SEC and ^{1}H NMR analyses, the extracted free copolymers had high molecular weights and included relatively smaller amounts of St-unit in the copolymer chains than those in the feed ratios (Table 1). According to the r_{St} and r_{MMA} values of 0.52 and 0.46, respectively,[15] the St-unit contents in copolymers should be richer than in the feed ratios of St monomer. Thus, it is considered that the surfaces, including interlayer surfaces, of the silicate layers affect the copolymerization kinetics of St and MMA (Scheme 1).

The results of the simultaneous copolymerization showed that effectively exfoliated nanocomposites with high St-unit contents of 75.0−90.6 unit % were obtained. Because of the relatively poor ability of St to make the MMT exfoliate, a higher St content tended to require a larger amount of copolymer for exfoliation.

To achieve both the exfoliation of the silicate layers and high St content in the composite, a block copolymer having a short MMA block segment, which could function effectively in delaminating silicate layers, was prepared in situ. One of advantages of the VASP method, compared with the liquid phase reaction, is the easy exchange of the gaseous monomer,

Table 2. Consecutive VASP of Vinyl Monomers on AIBN Pre-intercalated C18MMT[a]

	monomer (mL)									
entry	1st MMA	2nd St	temp (°C) 1st/2nd	time (h) 1st/2nd	product (mg)	polymer yield (mg)	M_n[b] ($\times 10^5$)	PDI	*d*-spacing (nm)	unit ratio in copolymer[c] [St]/[MMA]
6	1	2	60/80	18/11	550	450	6.8	2.2	>4.4[d]	5.0

[a] Polymerization conditions: substrate, C18MMT (100 mg); C18MMT:AIBN = 30:1 (w/w). [b] Number-average molecular weight determined by SEC relative to polystyrene standards. [c] Calculated from ^{1}H NMR peak intensities of a singlet at 2.00−3.65 ppm (−$COOCH_3$ in MMA unit) and signals at 6.28−7.20 ppm (aromatic protons in St unit) in ^{1}H NMR spectra. [d] No diffraction peak in a range of 2θ = 2°−10°, which is indicative of exfoliated structure.

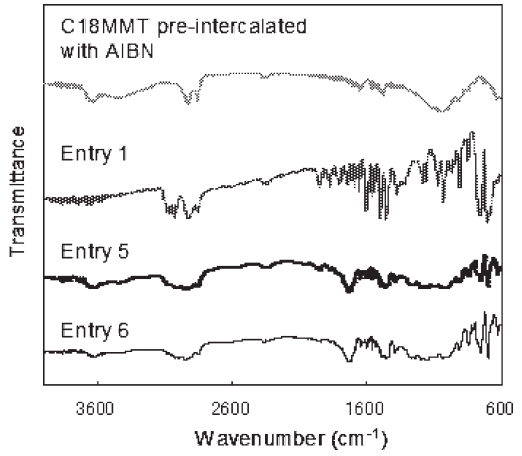

Figure 2. FTIR spectra of AIBN preintercalated C18MMT and PSt-based copolymer/C18MMT composites.

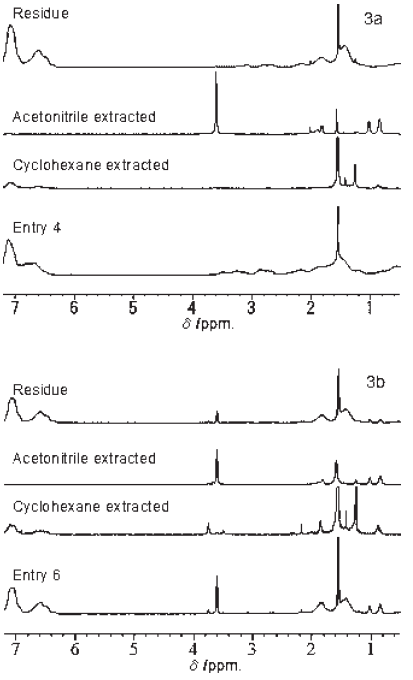

Figure 3. ^{1}H NMR spectra of the simultaneous and consecutive VASP products and their fractions isolated by a selective solvent extraction method: (a) simultaneous VASP product (entry 4); (b) consecutive VASP product.

whereby a block copolymer can be facilely produced by consecutive VASP.[11d] To construct a exfoliated nanocomposite comprising MMT and a styrene-based copolymer, the consecutive VASP of MMA and St was carried out in a two-step polymerization on the AIBN-pretreated C18MMT. The consecutive VASP smoothly proceeded by the first and second steps for MMA and St, respectively, to give powdery products (entry 6 in Table 2). From ^{1}H NMR analysis, the composition of the obtained product was rich in St-unit (83.3%) and had a high MMT content (18.2 wt %), achieving an effective expansion in the *d*-spacing between silicate layers (>4.4 nm in Figure 1).

Characterization of Copolymers. The as-polymerized products on the C18MMT surface were characterized by FTIR and ^{1}H NMR in Figures 2 and 3, respectively. FTIR spectra of poly(MMA-*ran*-St) (entry 5) and poly(MMA-*block*-St) (entry 6) showed characteristic peaks assigned to $\delta_{Ar-CH,out\ of\ plane}$ at 760 and 700 cm^{-1} and to $\nu_{C=O}$ at 1747 cm^{-1} for St and MMA components, respectively. The $\nu_{C=O}$ peaks were broader than the same peak of pure PMMA, indicating a hydrogen-bonding interaction between the surface of silicate layers and MMA-units in the intercalated polymer chains.[16] These results suggest that MMA-units in the copolymer chains are adsorbed and restricted in mobility on the platelet surface. On the other hand, no broadening of the peaks of $\delta_{Ar-CH,out\ of\ plane}$ was observed for both the products, suggesting no interaction between the St-unit and the silicate surface occurred.

To confirm compositions of copolymers formed by simultaneous and consecutive VASP, free polymers in the composites (entries 4 and 6) were extracted by THF at 80 °C for 24 h. A 92.7 wt % of the accumulated product in entry 4 was extracted as the free polymer. Thus, at least 7.3 wt % of the accumulation must be grafted on the substrate surfaces.[14] Fractionation of the THF-extracted component was carried out by a selective extraction method using particular solvents for both homopolymers, i.e., cyclohexane for PSt and acetonitrile for PMMA at 80 °C for 24 h. After the selective extraction, the residual copolymers were dissolved in a common solvent: chloroform. Each fraction was characterized with ^{1}H NMR and SEC. Results are listed in Table 3. It was found that the simultaneous VASP product (entry 4) comprised copolymer (71.9%) and both homopolymers of PSt (3.0%) and PMMA (25.1%). On the other hand, the consecutive VASP (entry 6) gave a product comprising high molecular weight St-rich copolymer (49.7%), low molecular weight St-rich copolymer (37.2%), and high molecular weight MMA homopolymer (13.1%). The MMA homopolymer obtained by consecutive VASP might be produced as terminated and/or occluded chains under accumulated chains before the delivery of the St monomer.[11d] These compositions must be reflected in copolymer chains combined with silicate surfaces.[14]

To confirm the first-order structure of VASP products, the isolated free polymers were analyzed by ^{1}H NMR. In Figure 3a,b, ^{1}H NMR spectra of the fractions isolated from the simultaneous and consecutive VASP products, entries 4 and 6, are shown together with the mixed product before fractionation. In Figure 3a, the ^{1}H NMR spectrum of the acetonitrile extracted fraction (PMMA) showed a sharp singlet signal at 3.6 ppm assigned to −$COOCH_3$ in

Table 3. Composition of Free Polymers Fractionated by Selective Solvents[a]

	cyclohexane extracted					acetonitrile extracted					chloroform soluble				
		(unit %)[b]					(unit %)[b]					(unit %)[b]			
entry	(wt %)	St	MMA	M_n[c]	PDI	(wt %)	St	MMA	M_n[c]	PDI	(wt %)	St	MMA	M_n[c]	PDI
4	3.0	100	0	6.4×10^5	2.5	25.1	0	100	5.5×10^5	2.4	71.9	81.3	18.7	5.6×10^5	2.1
6	37.2	88.8	11.2	8.0×10^4	1.3	13.1	0	100	4.6×10^5	2.1	49.7	82.2	17.8	8.5×10^5	2.0

[a] Extraction for 24 h at 80 °C. [b] Calculated from peak intensities of a singlet at 2.00−3.65 ppm (−$COOCH_3$ in MMA unit) and signals at 6.28−7.20 ppm (aromatic protons in St unit) in ^{1}H NMR spectra. [c] Calculated from SEC profile monitored with RI detector on the basis of PSt standards.

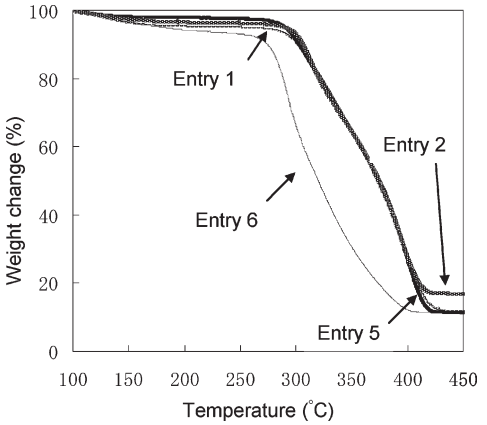

Figure 4. TG profiles of PSt/C18MMT (entry 1), poly(MMA-*ran*-St)/C18MMT (entries 2 and 5), and poly(MMA-*block*-St)/C18MMT (entry 6). Heating rate: 10 °C min^{-1} under N_2 flow (100 mL min^{-1}).

a continuous MMA-unit sequence. However, in the spectra of the cyclohexane extracted (PSt) and residual chloroform soluble (copolymer) fractions, there was no evidence of any sharp peak at 3.6 ppm, indicating that the MMA-unit was randomly distributed in the copolymer sequence. All the fractions in Figure 3b show the typical peak patterns as found with homopolymers and their block copolymer, clearly indicating the production of poly(MMA-*block*-PSt). Characteristic signal patterns of aromatic protons over the range of δ 6.3−7.2 ppm indicate a continuous St-unit sequence,[17−21] resulting from the large amount of St-unit, which forms the majority unit in the copolymer sequence.

From the above results, it is considered that the products prepared from the simultaneous and consecutive VASP of MMA and St are random and block copolymers, respectively. Although these are St-rich copolymers incorporating the MMA-units as a minor component, the minor MMA-units effectively function to delaminate the silicate layers during VASP. The characteristics of simplicity and effectiveness in such nanocomposite preparation are attractive attributes of VASP in addition to its features of being solventless and free in the prehomogeneous process.

Thermal Property and Morphology of Melt-Processed Composites. Thermogravimetric (TG) profiles of PS/C18MMT (entry 1), poly(MMA-*ran*-PS)/C18MMT (entries 2 and 5), and poly(MMA-*block*-PS)/C18MMT (entry 6) are shown in Figure 4. The TG profiles of entries 1, 2, and 5 exhibited similar multistep weight loss curves, reflecting the degradation behavior of the PSt homosequence. On the other hand, in spite of the similar molecular weight and MMA-unit content, the TG profile of the block copolymer/C18MMT (entry 6) showed rapid degradation at temperatures lower than those for the other samples. MMA is well-known as an easily depolymerizable polymer,[22] and it has been reported previously that a PMMA/C18MMT degraded in a similar temperature range.[14] Thus, the rapid thermal degradation of

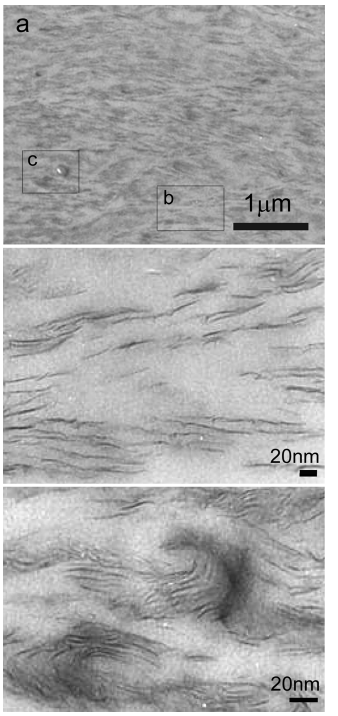

Figure 5. TEM images of melt-pressed poly(MMA-*ran*-St)/C18MMT nanocomposite thin film (entry 3) at (a) low and high magnifications of (b) exfoliated and (c) intercalated parts.

poly(MMA-*block*-St)/C18MMT (entry 6) must be ascribed to the easy degradation of the long PMMA segment in the block copolymer.

To determine the homogeneous dispersion of individual silicate platelets in the PSt-based polymer matrix, TEM images of the obtained nanocomposite were observed after melt-processing of the products at 210 °C for 2 min. Typical TEM images of the poly(MMA-*ran*-St)/MMT/C18MMT (entry 3) melt-pressed film at low and high magnifications are shown in Figure 5.[23,24] In the low-magnification image (Figure 5a), it seems that the MMT is distributed in a relatively homogeneous manner, showing mostly exfoliated silicate platelets in the polymer matrix. However, in some small areas intercalated structures are also found (Figure 5c). Even after melt-processing, the effectively delaminated morphology of the silicate platelets was preserved without relamination. This suggests that the polymer chains attached onto the silicate surfaces act to preserve the dispersion of individual silicate platelets in the polymer matrix.[14]

Therefore, the layered structure of MMT was effectively delaminated by the MMA-units in the copolymers during the VASP process, and the intercalated/exfoliated silicate platelets were dispersed homogeneously in a PSt-based polymer matrix, retaining the dispersed state even after the melt-processing of the nanocomposites.

Conclusions

PSt-based copolymer/MMT nanocomposites were successfully prepared by simultaneous and consecutive VASP of St and MMA. The advantages of the VASP technique: solventless nature and effectiveness, compared with an authentic liquid process, were determined through the preparation of intercalated/exfoliated nanocomposites. In the case of VASP of St on C18MMT, in spite of having the high polymer yield and molecular weight of the polymer component, C18MMT was only intercalated but not exfoliated. The effective exfoliation of the silicate layers was achieved by the simultaneous VASP of St and MMA. With increase in the MMA-unit content in the obtained random copolymers, the delamination of silicate layers effectively proceeded, resulting in the production of nanocomposite with high MMT content. This phenomenon must be induced by the particular interaction between a small amount of MMA-units in copolymer chains and silicate surfaces as suggested from the broadening of the $\nu_{C=O}$ absorption band of MMA-unit. To make the specific compatibility of MMA-unit with silicate surface function effectively, a block copolymer was synthesized, and the individual functions of its monomeric units, i.e., the delamination of silicate layers by MMA-units and the affinity with polymer matrices by St-units in the copolymers, were determined.

This approach allows the nanocomposites with accompanying effective exfoliation of silicate layers to be applied to a wide range of vaporizable monomers, which in the absence of this technique would be otherwise difficult to individually prepare.

Acknowledgment. This work was performed under the sponsorship of Henkel KGA in Germany. We thank PS Japan Corp. for providing the transmission electron micrograph.

References and Notes

(1) Tiwari, R. R.; Natarajan, U. *Polym. Int*. **2008**, *57*, 738–743.
(2) Mohammad, R. K.; Jeong, H. Y. *J. Polym. Sci., Part B: Polym. Phys*. **2008**, *32*, 2279–2285.
(3) Uthirakumar, P.; Nahm, K. S.; Hahn, Y. B.; Lee, Y. S. *Eur. Polym. J*. **2004**, *40*, 2437–2444.
(4) (a) Weimer, M.; Chen, H.; Giannelis, E. P.; Sogah, D. Y. *J. Am. Chem. Soc*. **1999**, *121*, 1615–1616. (b) Di, J.; Sogah, D. Y. *Macromolecules* **2006**, *39*, 1020–1028. (c) Di, J.; Sogah, D. Y. *Macromolecules* **2006**, *39*, 5052–5057.
(5) Hoffmann, B.; Dietrich, C.; Thomann, R.; Friedrich, C.; Muehaupt, R. *Macromol. Rapid Commun*. **2000**, *21*, 57–61.
(6) Zhao, J.; Morgan, A. B.; Harris, J. D. *Polymer* **2005**, *46*, 8641–8660.
(7) Akelah, A.; Moet, M. *J. Mater. Sci*. **1996**, *31*, 3589–3596.
(8) Camerani, M.; Lelle, M.; Sparanacci, K.; Sandrolini, F.; Franxescangeli, O. *J. Mater. Sci*. **1998**, *33*, 2883–2888.
(9) Park, C. I.; Choi, W. M.; Kim, M. H.; Park, O. O. *J. Polym. Sci., Part B: Polym. Phys*. **2004**, *42*, 1685–1693.
(10) (a) Huang, X.; Brittain, W. J. *Macromolecules* **2001**, *34*, 3255–3260. (b) Fan, X.; Xia, C.; Advincula, R. C. *Langmuir* **2003**, *19*, 4381–4389. (c) Fan, X.; Xia, C.; Advincula, R. C. *Langmuir* **2005**, *21*, 2537–2544.
(11) (a) Fu, D.; Weng, L.-T.; Du, B.; Tsui, O. K. C.; Xu, B. *Adv. Mater*. **2002**, *14*, 339–343. (b) Wang, Y.; Chang, Y. C. *Adv. Mater*. **2003**, *15*, 290–293. (c) Gu, H.; Xu, C.; Weng, L.-T.; Xu, B. *J. Am. Chem. Soc*. **2003**, *125*, 9256–9257. (d) Yasutake, M.; Hiki, S.; Andou, Y.; Nishida, H.; Endo, T. *Macromolecules* **2003**, *36*, 5974–5981. (e) Chan, K.; Gleason, K. K. *Langmuir* **2005**, *21*, 8930–8939. (f) Lau, K. K. S.; Gleason, K. K. *Adv. Mater*. **2006**, *18*, 1972–1977. (g) Andou, Y.; Nishida, H.; Endo, T. *Chem. Commun*. **2006**, 5018–5020. (h) Andou, Y.; Yasutake, M.; Nishida, H.; Endo, T. *J. Photopolym. Sci. Technol*. **2007**, *20*, 523–528.
(12) Nishida, H.; Yamashita, M.; Andou, Y.; Jeong, J.-M.; Endo, T. *Macromol. Mater. Eng*. **2005**, *290*, 848–856.
(13) (a) Lau, K. K. S.; Bico, J.; Teo, K. B. K.; Chhowalla, M.; Amaratunga, G. A. J.; Milne, W. I.; McKinley, G. H.; Gleason, K. K. *Nano Lett*. **2003**, *3*, 1701–1705. (b) Gupta, M.; Kapur, V.; Pinkerton, N. M.; Gleason, K. K. *Chem. Mater*. **2008**, *20*, 1646–1651.
(14) Andou, Y.; Jeong, J.-M.; Hiki, S.; Nishida, H.; Endo, T. *Macromolecules* **2009**, *42*, 768–772.
(15) Greenley, R. Z. Free radical copolymerization reactivity ratios. In *Polymer Handbook*, 4th ed.; Brandrup, J., Immergut, E. H., Grulke, E. A., Eds.; Wiley-Interscience: New York, 1999; pp II/181−308.
(16) Zhao, Q.; Samulski, E. T. *Macromolecules* **2005**, *38*, 7967–7971.
(17) Zhang, H.; Hong, K.; Mays, J. W. *Macromolecules* **2002**, *35*, 5738–5741.
(18) Narita, H.; Kinoshita, H.; Araki, T. *J. Polym. Sci., Part A: Polym. Chem*. **1992**, *30*, 333–335.
(19) Harwood, H. J.; Ritchey, W. M. *Polym. Lett*. **1965**, *3*, 419–426.
(20) Ito, K.; Yamashita, Y. *J. Polym. Sci*. **1965**, *B3*, 625–630.
(21) Kwon, T. S.; Kondo, S.; Kunisada, H.; Yuki, Y. *Polym. J*. **1998**, *30*, 559–565.
(22) Ferriol, M.; Gentilhomme, A.; Cochez, M.; Oget, N.; Mieloszynski, J. L. *Polym. Degrad. Stab*. **2003**, *79*, 271–281.
(23) Morgan, A. B.; Gilman, J. W. *J. Appl. Polym. Sci*. **2003**, *87*, 1329–1338.
(24) Vermogen, A.; Masenelli-Varlot, K.; Seguela, R.; Duchet-Rumeau, J.; Boucard, S.; Prele, P. *Macromolecules* **2005**, *38*, 9661–9669.